Ultrasound-Alkali-Assisted Isolation of Cellulose from Coconut Shells

Pavitra Mohan,[a] Nor Saadah Mohd Yusof,[a,b] Sabu Thomas,[c] and Nor Mas Mira Abd Rahman [a,*]

This research explored the isolation of cellulose from coconut shells using ultrasound. It involved two types of cellulose isolation: alkali and bleached cellulose (ABC) and ultrasound-alkali-assisted isolated cellulose (UAIC). The products were characterized using various techniques, including attenuated total reflection-Fourier transform infrared spectroscopy (ATR-FTIR), X-ray diffraction analysis (XRD), thermogravimetric analysis (TGA), and field emission scanning electron microscopy (FESEM). The ATR-FTIR results confirmed the effective removal of lignin and hemicellulose in the ABC and UAIC samples. Field emission scanning electron microscopy analysis revealed the production of micro-sized cellulose. The TGA and XRD results showed improved thermal stability and crystallinity in ABC and UAIC, attributed to the elimination of non-cellulosic constituents. However, the thermal stability and crystallinity of UAIC were lower compared to ABC, likely due to the cavitation effect caused by sonication. The findings suggest that ultrasonication is an efficient and promising method for isolating cellulose.

DOI: 10.15376/biores.19.4.7870-7885

Keywords: Cellulose; Ultrasound assisted isolation; Ultrasonication; Alkali treatment; Bleaching

*Contact information: a: Department of Chemistry, Faculty of Science, Universiti Malaya, 50603 Kuala Lumpur; b: Universiti Malaya Centre for Ionic Liquids (UMCiL) Universiti Malaya, 50603 Kuala Lumpur; c: School of Chemical Sciences, Mahatma Gandhi University, Priyadarshini Hills P.O. Kottayam, 686560, Kerala, India; *Corresponding author: nmmira@um.edu.my*

INTRODUCTION

Cocos nucifera, more commonly known as coconut, is a vital food and oil source that has been grown in over 90 countries (Jerard *et al.* 2018). Coconut is one of the most consumed products in the world, with approximately 5 kg per capita of coconuts consumed annually. However, this high consumption results in significant coconut waste, especially the coconut shell material. Coconut shell is one of the many valuable lignocellulosic biomass residues. It is the non-edible component of the coconut. It is mainly composed of hemicellulose, cellulose, and lignin (Rizal *et al.* 2020; Kalla *et al.* 2022). While coconut shells are biodegradable, they are remarkably durable and strong, leading to an extended biodegradation process. Coconut shells are often discarded or burned, both of which present environmental challenges. Disposing of coconut shells in landfills contributes to landfill issues, as they take a long time to break down and can accumulate in landfills. Burning them, on the other hand, leads to air pollution. Rather than discarding or burning coconut shells, they can serve as valuable sources of cellulose for various industries, including cosmetics, pharmaceuticals, and the food industry.

Although there are a plentiful and renewable resource with a lot of promise, coconut

shells have historically been regarded as waste material with little commercial utility. Because coconut shells are readily available and have a high cellulose content, they are a desirable source for cellulose production, particularly in areas where coconuts are plentiful (Nayar 2017). Utilising coconut shells also complies with waste valorisation and sustainable development concepts, turning trash into useful products.

Cellulose has been gaining significant attention globally due to its high availability, biodegradability, and unique physical and chemical properties, which makes it suitable for a variety of applications such as biofuel production and fillers in the pharmaceutical industry (Shokri and Adibkia 2013; Gupta *et al.* 2019).

In plants and trees, photosynthesis produces cellulose. It is considered the most abundant resource of renewable polymers on earth and is the main source for the replacement of oil-based feedstocks (Chen *et al.* 2015). Cellulose has an unbranched chain with high crystallinity and polymerization degree (Pasquini *et al.* 2010). The cellulose molecule has a length of up to several micrometers (Gardner *et al.* 2008). Cellulose is present in an amorphous form in the plant fiber linked by intermolecular and intramolecular hydrogen bonds to the crystalline phase.

Cellulose is commonly isolated using alkali and bleaching treatments. This method involves treating the lignocellulosic biomass with an alkali such as sodium hydroxide, followed by bleaching with sodium chlorite and acetic acid to remove the non-cellulosic components such as hemicellulose, lignin, and impurities. The bleaching also ensures a high purity of isolated cellulose (Ouarhim *et al.* 2019).

Although conventional isolation techniques are well-established, in order to degrade the lignocellulosic structure of biomass such as coconut shells, they frequently need strong chemicals, high temperatures, and prolonged reaction periods (Javanmard *et al.* 2024). This contributes to both the operational costs and negative environmental effects due to the need for extensive chemical recovery systems. Research has indicated that the high lignin content and compact structure of coconut shells (Rizal *et al.* 2020) make them particularly resistant to conventional isolation techniques making the isolation of cellulose difficult. An alkali-assisted ultrasound isolation method was employed in this study to isolate cellulose. Ultrasound is a multipurpose energy applied in a variety of disciplines, including health, navigation, and industrial. This energy is used in industrial processes, including homogenization, emulsification, isolation, crystallization, degassing, defoaming, and cleaning. Ultrasound has several advantages in these operations, especially in the isolation of cellulose compared to conventional isolation techniques. Ultrasound-assisted isolation reduces the need for harsh chemicals and improves the yield and quality of the isolated cellulose, making it a more environmentally friendly and energy-efficient method. Ultrasound's mechanical effects, such as cavitation, improves mass transfer and hasten the lignocellulosic matrix's breakdown, which is less possible with conventional techniques (Rodrigues and Pinto 2007; Lavilla and Bendicho 2017).

Despite the many potentials of cellulose, there is a lack of research exploring the isolation of cellulose from coconut shells. Using ultrasound to investigate coconut shells as a cellulose source is a novel strategy that may lead to new directions in both industrial and scientific applications. While the potential of other biomass sources, such as empty palm fruit bunches, has been well investigated, investigating the possibilities of coconut shells may reveal novel material qualities and uses.

Even though there are studies that have used coconut shells to isolate cellulose (Kalla *et al.* 2022), the application of ultrasound for the isolation of this material is insufficient. Therefore, the current study aimed to isolate and compare the properties of

cellulose from coconut shells using alkali and bleaching treatment and ultrasound-assisted treatment with alkali. Attenuated total reflection-Fourier transform infrared spectroscopy (ATR-FTIR), field emission scanning electron microscopy (FESEM), X-ray diffraction (XRD), and thermogravimetric analysis (TGA) were used to characterize the isolated cellulose and analyze their properties.

EXPERIMENTAL

Materials

Coconut shells were collected from a local grocery store, while the chemicals used were commercially available. Toluene (99.5%), ethanol (95%), and 80% sodium chlorite ($NaClO_2$) were purchased from Sigma Aldrich, sodium hydroxide (NaOH) was purchased from Emsure, and glacial acetic acid (CH_3COOH) was purchased from J.T. Baker. All chemicals were of reagent grade and used as received without further purification.

Methods

Pretreatment of raw coconut shell fiber (RCSF)

The raw coconut shell was dried and ground into powder using a high-speed multi-function mill in order to decrease the particle size and enhance the surface area of the coconut shells and allow for more efficient chemical penetration during the isolation. The obtained powder was sieved using a 35-mesh sieve and dried until a consistent weight was achieved. This material was referred to as raw coconut shell fiber (RCSF). To remove impurities such as wax and extractives, the RCSF was subjected to Soxhlet extraction for 6 h using a mixture of toluene and ethanol in a 2:1 ratio. The coconut shell powders were subsequently termed Soxhlet extracted coconut shell fiber (SCSF).

Cellulose isolation from SCSF: Alkali delignification and bleaching treatment purification

The sample was treated with 1 M NaOH for 4 h at 80 °C to remove hemicellulose. The resulting residue was filtered and washed multiple times with distilled water until the filtrate reached a neutral pH. Following the alkali treatment, the bleaching method was used to remove lignin. The alkali-treated sample was heated in 150 mL of water with 1.5 g of sodium chlorite and 27 drops of glacial acetic acid for one h at 80 °C. The process was repeated 11 times. Finally, the residue was filtered and rinsed with distilled water until a neutral filtrate was obtained. This experiment was repeated 3 times and the standard deviation obtained was 0.141. The obtained sample was referred to as ABC (alkali and bleached cellulose).

Cellulose isolation from SCSF: ultrasound-assisted alkali treatment

The coconut shell powder was treated with 1 M NaOH solution at room temperature while being exposed to ultrasonic irradiation at 30% sonication power out of 500 W, which is 150 W, for 30 min at room temperature. The sonication was conducted using continuous mode with continues flow of water to avoid temperature increase. The ultrasonication was performed using a 1.0 cm tip diameter probe, with the depth kept constant at 4 cm. After the sonication, the mixture was constantly stirred for 2 h at 80 °C. The residue was filtered and thoroughly washed with water until a neutral filtrate was obtained. The isolated cellulose was dried until a consistent weight was achieved. This experiment was repeated 3 times and the standard deviation obtained was 0.173. The resulting sample was termed

UAIC (ultrasound-assisted isolated cellulose).

Characterizations

Yield

The yield of each isolated cellulose was calculated using Eq. 1 and 2 to obtain the average yield,

$$\text{Yield (\%)} = \frac{m_f}{m_i} \times 100\% \quad (1)$$

$$\text{Average yield} = \frac{\sum \text{Yield (\%)}}{3} \quad (2)$$

where m_f is the final mass (mass of cellulose), and m_i is the initial mass of sample (SCSF) used in g.

Attenuated total reflection-Fourier transform infrared spectroscopy (ATR-FTIR) analysis

Fourier transform infrared spectrometry analysis was carried out to observe changes in functional groups resulting from different treatments. Attenuated total reflection-Fourier transform infrared spectroscopy (ATR-FTIR) was used to record the FTIR spectra in the transmittance mode, covering a range from 400 to 4000 cm^{-1}.

Field emission scanning electron microscopy (FESEM) analysis

Field emission scanning electron microscopy analysis was used to study the morphology of the samples. To prepare the sample for analysis, a small amount of sample was placed on a glass grid. The samples were vacuum-dried and sputter-coated with platinum before FESEM analysis. The size distribution was obtained by measuring the size of 150 particles using *ImageJ* software.

X-ray diffraction (XRD) analysis

X-ray diffraction analysis was conducted to evaluate the crystallinity of the samples. The samples were characterized using an X-ray diffractometer. The diffracted intensity of Cu Kα radiation (λ = 0.154 nm) was measured in a 2θ range between 10° and 70°. The generator was operated at 40 kV and 20 mA. The crystallinity index was calculated according to the Segal's equation (Segal *et al.* 1959),

$$\text{CI (\%)} = \frac{I_{200} - I_{am}}{I_{200}} \times 100\% \quad (3)$$

where I_{200} is the highest intensity of the lattice diffraction peak, which occurs at approximately 22 to 23°, and I_{am} is the minimum intensity of the amorphous region of the sample, which occurs at about 18°.

Thermogravimetric (TGA) analysis

The thermogravimetric analysis was used to provide information on the thermal stability of the samples. The samples were subjected to thermogravimetric analysis by heating 1 mg of each sample from 30 to 900 °C under a nitrogen atmosphere with a heating rate of 10 °C min^{-1} and a flow rate of 20 mL min^{-1}. The thermogravimetric analysis provides data on how samples and their masses respond to the increasing temperature applied.

RESULTS AND DISCUSSION

Yield of Cellulose

After each treatment, the quantification of cellulose yields was calculated using Eq. 1, and the average yield was calculated using Eq 2. The UAIC treatment had a significantly higher yield of cellulose (65.3%) compared to ABC (24.7%). The lower yield of ABC can be attributed to the repetitive process and the high-temperature bleaching treatment, resulting in cellulose degradation and decomposition.

The increased yield of UAIC is attributed to the cavitation phenomenon from sonication. During ultrasonication, the high-frequency sound waves create cavitation bubbles, which expand to their maximum expansion size and asymmetrically collapse near the RCSF surface. This generates intense localized forces known as microjet, which disrupt the cell wall of the RCSF, leading to the release of cellulose from the plant material. The advantage of ultrasound lies in its ability to enhance the accessibility of NaOH to the cellulose through increased mass transfer. It also enhances the breakdown of lignin and hemicellulose components within the RCSF (Chemat *et al.* 2016; Yi *et al.* 2019). Consequently, ultrasound-assisted isolation can give a higher yield of cellulose compared to conventional methods that rely solely on chemical treatments.

The alkali and bleaching treatment method also shares the aim of breaking down the cell wall of RCSF and degrading lignin and hemicellulose. Although this approach is efficient during cellulose isolation, cellulose yield may not be fully maximized due to limitations in the degree of breakdown or solvent accessibility to cellulose. In this instance, it is thought that ultrasound-assisted isolation provides additional mechanical disruption that improves the isolation of cellulose and, as a result, leads to a larger yield of cellulose.

ATR-FTIR

Attenuated total reflectance-Fourier transform infrared spectroscopy analysis was done to discern the changes in the cellulose's functional groups following the isolation process, particularly upon confirming the elimination of hemicellulose and lignin components (Wulandari *et al.* 2016). Figure 1 shows the FTIR spectra of RCSF, ABC, and UAIC.

The functional groups present in the isolated celluloses from coconut shell (ABC and UAIC spectra in Fig. 1) exhibited similarity to those identified in cellulose isolated from different raw materials, such as Agave angustifolia fibers, sugarcane bagasse, and oil palm empty palm fruit bunch fibers (Rosli *et al.* 2013; Ching and Ng 2014; Theivasanthi *et al.* 2018).

The FTIR spectra of ABC and UAIC shared similarities in terms of the peaks present. However, they can be distinguished by the slight change in peak intensities. This variation indicates a change in the crystallinity of the samples (Rosli *et al.* 2013). In Fig. 1, the intensity of the ABC peaks was lower compared to UAIC samples. The decrease in peak intensity indicates a decrease in crystallinity.

In the FTIR spectra of RCSF, ABC, and UAIC, the peak at 3336 cm^{-1} corresponds to the stretching vibration of OH groups in cellulose. The peak at 2878 cm^{-1} corresponds to the C-H stretching vibration. Cellulose is typically hydrophilic and has a strong interaction with water. This is indicated by the absorbance peak at 1619 cm^{-1} due to the O-H bending in the absorbed water (Evans *et al.* 2019). These observations highlight the structural similarities and water-interacting properties of the isolated cellulose samples in this study, consistent with cellulose isolated from different sources. The FTIR spectra

provide further insights into the composition of the isolated cellulose sample. The peaks around 1433, 1360, and 1318 cm^{-1} are attributed to CH_2 scissoring at C-6 in the crystalline region of cellulose, C-H bending, and CH_2 wagging at C-6 of the cellulose, respectively (Kumar *et al.* 2014). The peak at 1235 cm^{-1} represents C-OH in plane stretch at C-6, while the absorption peak at 1027 cm^{-1} is due to the C-O-C group of the pyranose skeletal ring (Melikoğlu *et al.* 2019; Cichosz and Masek 2020).

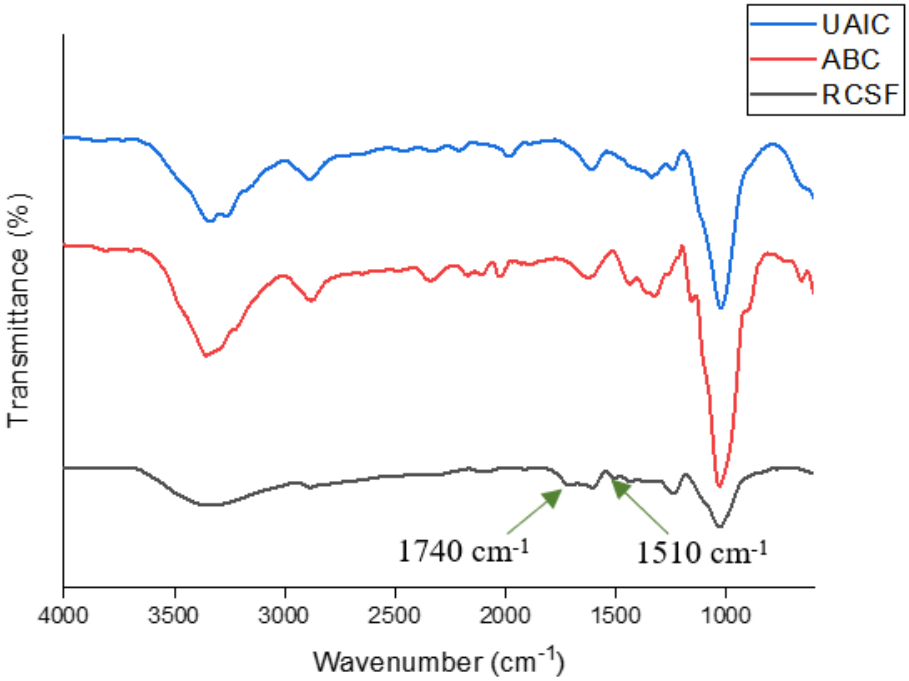

Fig. 1. FTIR spectra of Raw coconut shell fiber (RCSF) (black), Alkali and bleached cellulose (ABC) (red) and Ultrasound-alkali-assisted isolated cellulose (UAIC) (blue)

The C = O stretch of the acetyl and uronic ester group of hemicellulose ester, carbonyl ester linkage of the ferulic group, and p-coumaric monomeric lignin exhibit an absorption peak around 1740 cm^{-1} (Ching and Ng 2014). The peak at 1510 cm^{-1} represents the stretching of the aromatic ring of lignin. Referring to Fig. 1, these peaks are present in the FTIR spectra of RCSF but are notably absent in the FTIR spectra of ABC and UAIC. This absence serves as strong evidence that hemicellulose and lignin underwent degradation and were effectively eliminated during the chemical and ultrasonication treatments due to hemicellulose and lignin bond cleavage (Zhang *et al.* 2014). This supports the successful isolation and purification of cellulose from the coconut shell material.

Morphological Analysis

Field emission scanning electron microscopy analysis was conducted to examine the morphological characteristics, encompassing aspects such as the shape and size of isolated materials. For the accuracy of the observation, the samples were sputter coated with platinum during preparation to avoid charge accumulation. Figure 2 displays the FESEM images of raw coconut shell fiber (RCSF), alkali and bleached cellulose (ABC), and ultrasound-alkali-assisted isolated cellulose (UAIC).

The results revealed that RCSF exhibits bundles of fibers with varying sizes and irregular shapes alongside some isolated individual fibers. To provide a comprehensive

assessment of these materials, a size distribution analysis was conducted, based on the examination of 150 particles. The outcome of the size distribution analysis is visually presented in Figs. 3 and 4. The analysis results for size distribution are also summarized in Tables 1 and 2.

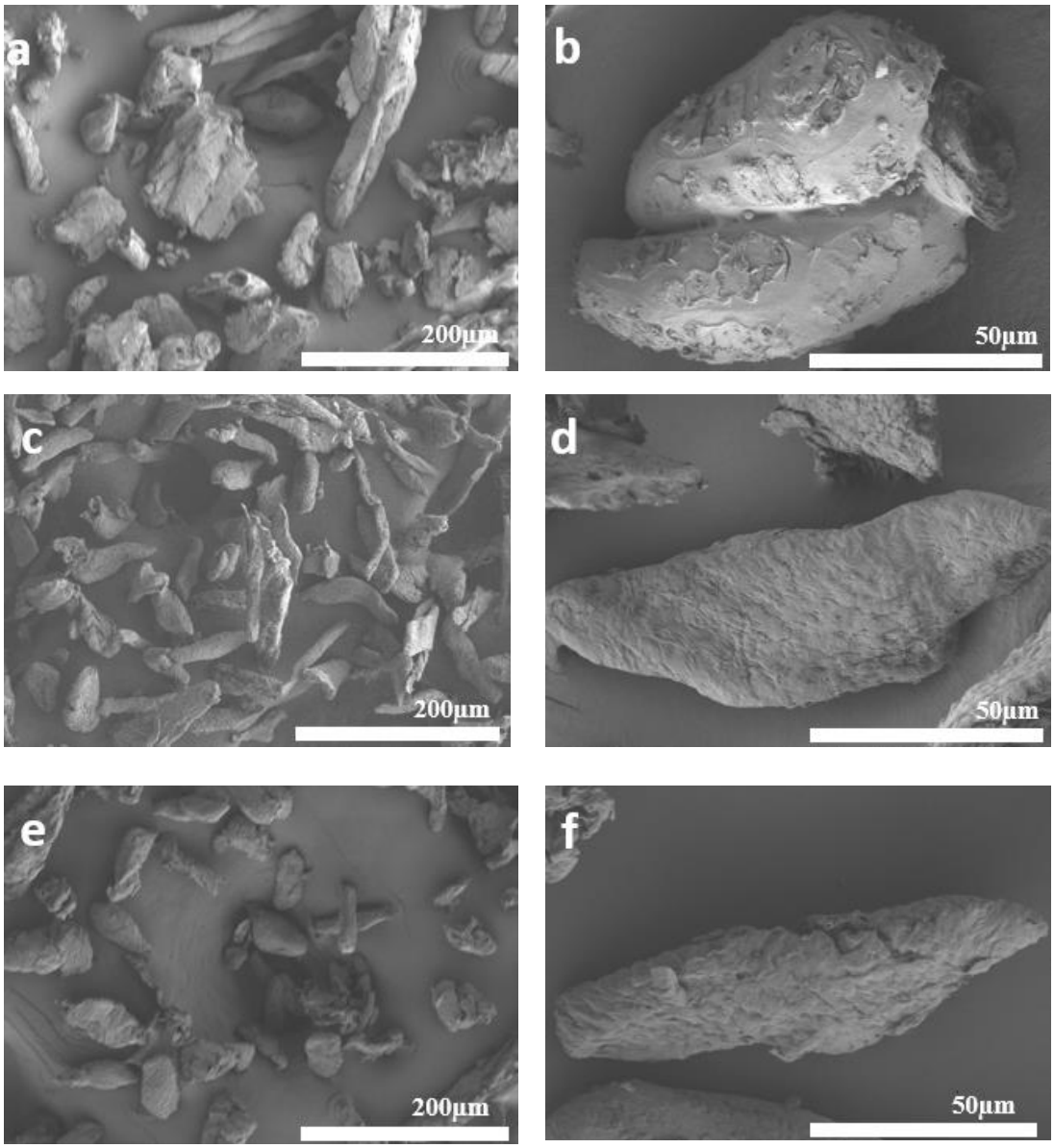

Fig. 2. FESEM images of a, b) Raw coconut shell fiber (RCSF) , c, d) Alkali and bleached cellulose(ABC) and e, f) Ultrasound-alkali-assisted isolated cellulose (UAIC) at different magnifications

The average length and diameter of ABC and UAIC were lower than that of the RCSF. The initial raw material contains non-cellulosic components such as lignin, hemicellulose, wax, and other impurities that act as cementing material, holding the fibers together in bundles. However, the application of alkali, bleaching, and ultrasonication treatments on the RCSF caused the removal of these non-cellulosic cementing materials by cleaving the bonds between hemicellulose and lignin. This effectively led to the fiber bundles separating into individual fibers with smaller average lengths and diameters. The

morphological alteration indicates the successful purification and processing of cellulose from the raw coconut shell fiber.

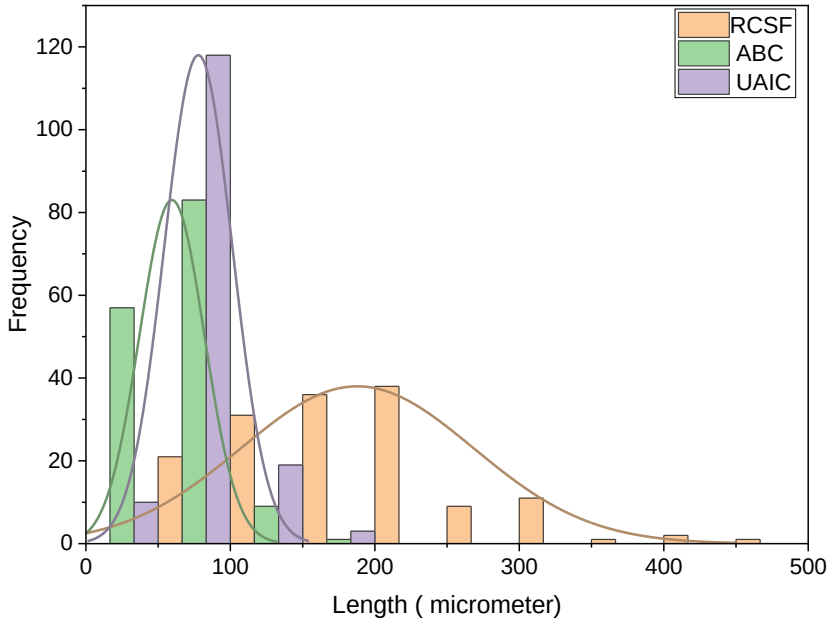

Fig. 3. Length distribution of Raw coconut shell fiber (RCSF), Alkali and bleached cellulose (ABC) and Ultrasound-alkali-assisted isolated cellulose (UAIC)

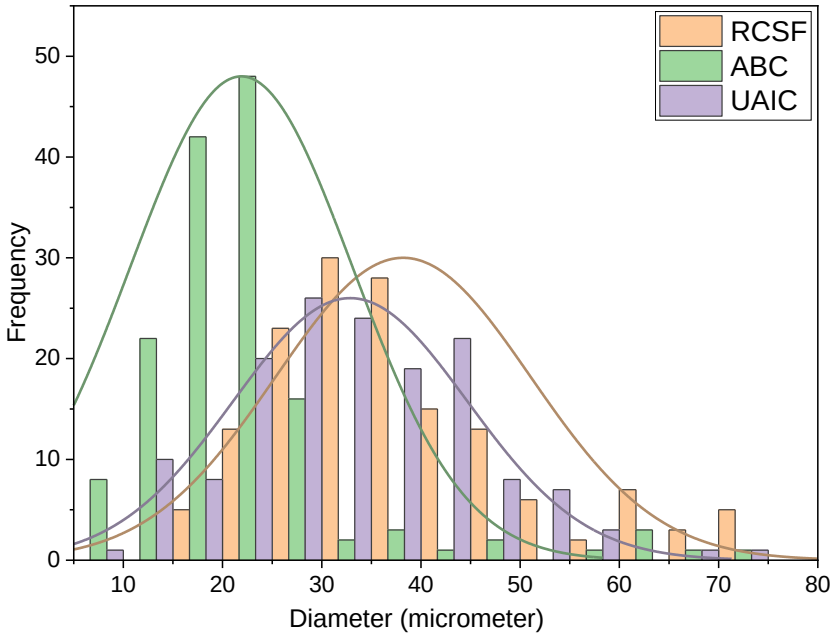

Fig. 4. Diameter distribution of Raw coconut shell fiber (RCSF), Alkali and bleached cellulose (ABC) and Ultrasound-alkali-assisted isolated cellulose (UAIC)

Table 1. Summary of Length of Particles for Raw Coconut Shell Fiber (RCSF), Alkali and Bleached Cellulose (ABC) and Ultrasound-Alkali-Assisted Isolated Cellulose (UAIC)

Sample	Length (µm)			
	Mean	Standard deviation	Minimum	Maximum
RCSF	187.84	80.57	57.28	471.90
ABC	59.53	22.49	14.01	157.40
UAIC	77.79	23.63	37.77	183.10

Table 2. Summary of Diameter of Particles for Raw Coconut Shell Fiber (RCSF), Alkali and Bleached Cellulose (ABC) and Ultrasound-Alkali-Assisted Isolated Cellulose (UAIC)

Sample	Diameter (µm)			
	Mean	Standard deviation	Minimum	Maximum
RCSF	38.20	12.85	16.77	74.87
ABC	22.57	13.99	6.51	67.45
UAIC	32.87	11.81	8.94	73.82

Moreover, there is a notable distinction in the surface morphology of ABC (Fig. 2d) and UAIC (Fig. 2f). Alkali and bleached cellulose and UAIC display a smoother surface and smaller size when compared to RCSF. The difference can be attributed to the effective removal of non-cellulosic components from the fibers by repeated bleaching with sodium chlorite. The FTIR analysis (Fig. 1) also confirms the removal of non-cellulosic components from ABC and UAIC. However, the UAIC shows a rougher and cracked surface, which can be attributed to the cavitation effect, specifically micro jetting during the asymmetrical implosion of microbubbles, as investigated by He *et al.* (2022). Previous research has demonstrated that the combined action of NaOH and ultrasound induces surface rupture and disintegration (He *et al.* 2022).

The results demonstrate that the isolation of cellulose from coconut shells can be achieved through ultrasound-assisted alkaline treatment. This process not only purifies the cellulose but also reduces particle size, presenting valuable insights for the potential applications of cellulose derived from this sustainable source.

XRD Analysis

X-ray diffraction analysis was conducted to examine the crystallinity index (C_i) of both the isolated cellulose. Figure 5 shows the XRD diffractogram of RSCF, ABC, and UAIC.

The XRD pattern of cellulose exhibited diffraction peaks at approximately 2θ = 18°, 22.5°, and 35.5°, corresponding to the planes of 110, 002, and 004, respectively. The intensity peaks at 110 represent the amorphous region of the sample while the intensity peaks at 002 and 004 represent crystalline regions of the samples. These peaks also indicate the presence of the crystallinity index (Ci) in all samples (Rosli *et al.* 2013). The intensity peaks at 38°, 44°, 65°, and 78° correspond to the silicon dioxide and silicon carbide in the RCSF. The absence of these peaks in the ABC and UAIC indicates that impurities and non-cellulosic components were removed from the raw material (Madakson *et al.* 2012). The Ci was calculated using Eq. 3 and is presented in Table 3.

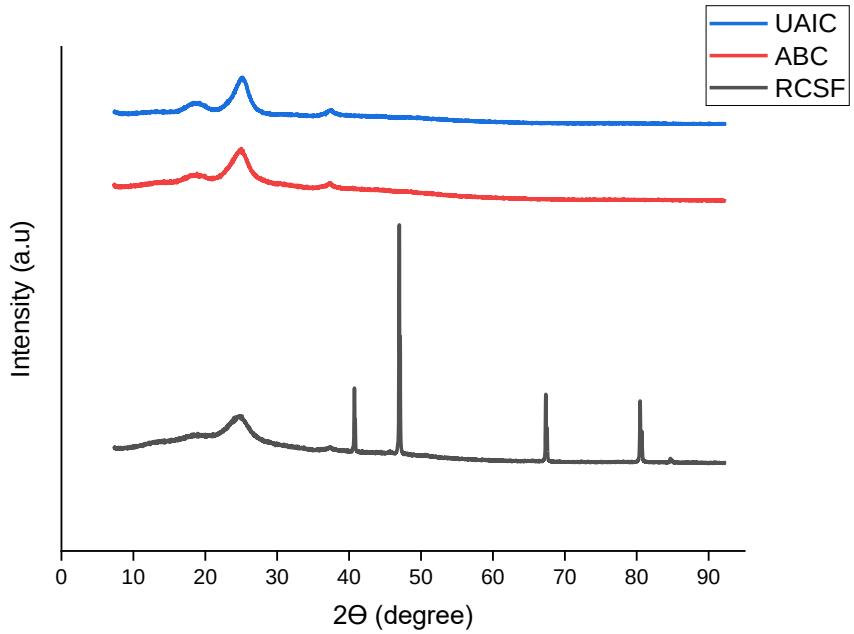

Fig. 5. X-ray diffraction diffractogram of raw coconut shell fiber (RSCF), alkali and bleached cellulose (ABC), and ultrasound-alkali-assisted cellulose (UAIC)

Table 3. Crystallinity Index of Raw Coconut Shell Fiber (RCSF), Alkali and Bleached Cellulose (ABC) and Ultrasound-Alkali-Assisted Isolated Cellulose (UAIC)

Sample	Ci (%)
RCSF	37.5
ABC	50.3
UAIC	46.5

The crystallinity of ABC (50.3%) and UAIC (46.5%) was higher than RCSF. The crystallinity increased in the order of RCSF < UAIC < ABC. The lower crystallinity index of RCSF can be attributed to amorphous non-cellulosic components, such as hemicellulose, lignin, and other impurities. These materials intertwine within the fibers, contributing to reduced crystallinity. Materials such as lignin and hemicellulose have lower crystallinity values since they are more amorphous than cellulose, which has both amorphous and crystalline regions. The crystallinity of RSCF was lower than ABC and UAIC. After the removal of the component with a lower crystallinity value, consequently, the crystallinity for ABC and UAIC was higher because they only consist of cellulose.

Therefore, removing these materials during alkali, bleaching, and ultrasonication treatments increased the crystallinity. However, the UAIC exhibited slightly lower crystallinity compared to ABC. This can be attributed to the fact that, during sonication, cavitation occurs, where the collapse of cavitating bubbles takes place. When this happens, the potential energy of the bubble is converted to kinetic energy that passes through the bubble and hits the opposite bubble at several hundred meters per second before hitting the fiber surface. This causes extreme damage at the point of impact, and the amorphous and crystalline regions are subjected to intense collision. Consequently, this causes fractures and damage to the crystalline part of the cellulose, ultimately reducing the crystallinity (Li *et al.* 2012).

TGA Analysis

TGA was conducted to evaluate the potential utility of cellulose for high-temperature applications (Liu *et al.* 2016). The TGA and DTG graphs of RCSF, ABC, and UAIC are shown in Figs. 6 and 7. Table 4 summarizes the degradation temperature range and percentage of weight loss in each degradation step of RCSF, ABC, and UAIC.

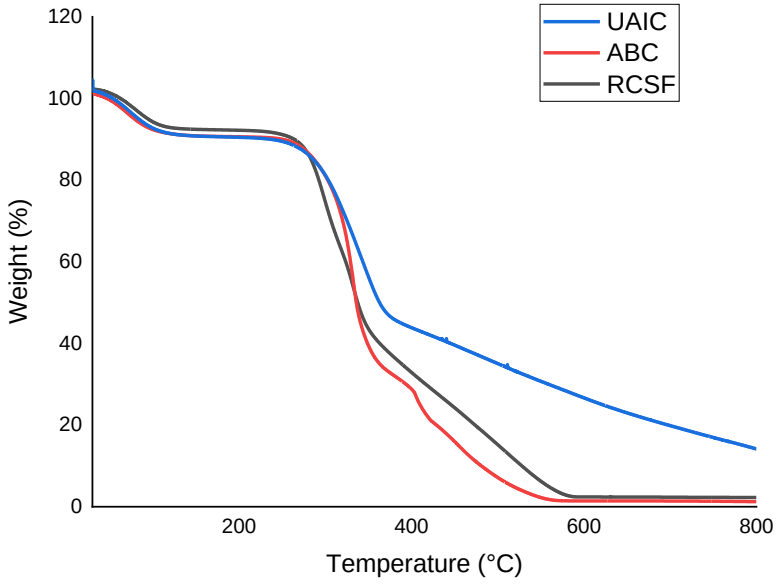

Fig. 6. Thermogravimetric analysis graph of Raw coconut shell fiber (RCSF), alkali and bleached cellulose (ABC), and ultrasound-alkali-assisted isolated cellulose (UAIC)

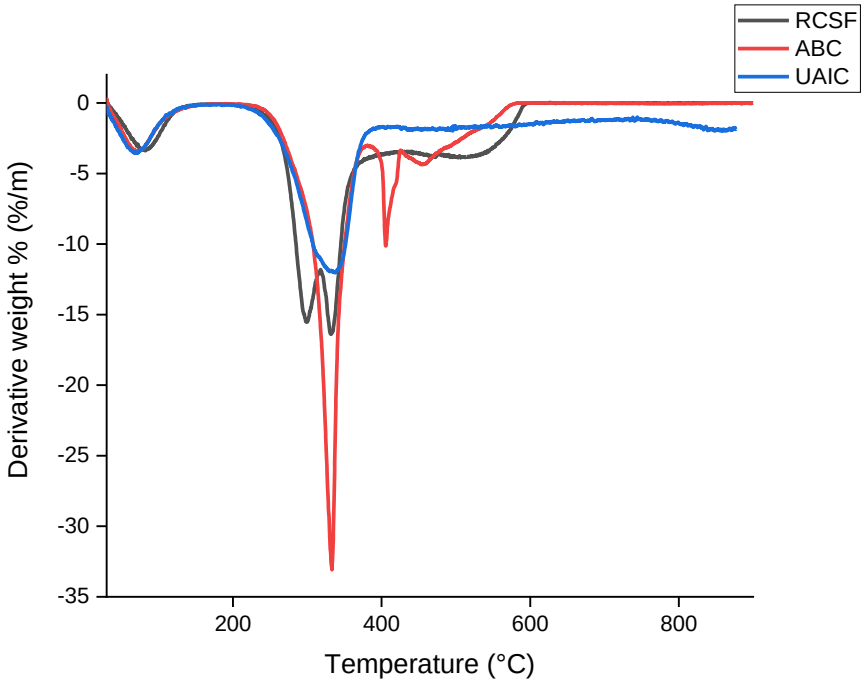

Fig. 7. Derivative thermogravimetry graph of raw coconut shell fiber (RCSF), akali and bleached cellulose (ABC), and ultrasound-alkali-assisted isolated cellulose (UAIC)

Table 4. Degradation Temperature Range and Weight Loss Percentage in Each Degradation Step of Raw Coconut Shell Fiber (RCSF), Alkali and Bleached Cellulose (ABC) and Ultrasound-Alkali-Assisted Isolated Cellulose (UAIC) Obtained from TGA and DTG Graphs

Degradation step / Sample	Step I		Step II		Step III	
	[a] Deg. temp. range (°C)	Weight loss (%)	[a] Deg. temp. range (°C)	Weight loss (%)	[a] Deg. temp. range (°C)	Weight loss (%)
RCSF	30-150	9.6	200-380	51.8	365- 590	37.2
ABC	30-140	9.6	240-380	58.3	380-560	30.5
UAIC	30-140	9.5	220-380	48.3	400-560	20.2

[a] Deg. temp. range represents degradation temperature range

The thermogravimetric analysis of RCSF in Figs. 6 and 7 reveals three degradation steps. The first degradation step occurred at 30 to 150 °C with a weight loss of 9.6%, which can be primarily attributed to moisture desorption and evaporation (Evans *et al.* 2019). The second degradation phase occurred within the range of 200 to 380 °C with a weight loss of about 51.8 %. In this stage, there were two distinct peaks. The first occurred within the range of 200 to 315 °C, corresponding to hemicellulose degradation, while the second occurred between 315 and 380 °C, which is consistent with cellulose degradation (Tangsathitkulchai *et al.* 2016). In general, the thermal decomposition of lignocellulosic biomass involves the degradation of its components; namely cellulose, hemicellulose, and lignin. Lignin degradation begins around 160 °C and continues over a wide temperature range up to 900 °C. On the other hand, hemicellulose degrades at lower temperatures, typically in the range of 200 to 315 °C, while cellulose decomposes at temperatures between 250 to 400 °C. The third degradation step occurred at 365 to 590 °C with a weight loss of about 37.2%, which can be attributed to the degradation of carbonic residue into components of low molecular weight and cleavage of glycosidic linkages in cellulose (Mohammed *et al.* 2021; Reddy *et al.* 2011). Similarly, the TGA and DTG graphs of both ABC and UAIC in Figs. 6 and 7 reveal three distinctive degradation phases. However, for the second step of thermal degradation for ABC and UAIC, there was only one peak observed. This thermal behavior can be attributed to the decomposition of cellulose (Bano and Negi 2017), which confirms the earlier removal of non-cellulosic components. Comparing with the RCSF, ABC and UAIC samples' degradation temperature at this stage started at a slightly higher temperature where the sample degraded at 200, 240, and 220 °C for RCSF, ABC, and UAIC respectively. The increased thermal degradation temperature of ABC and UAIC compared to RCSF is attributed to the removal of amorphous hemicellulose and lignin during the chemical treatments, which has been shown through FTIR analysis (Fig. 1). Additionally, the increased degradation temperature of ABC (240 °C) compared to UAIC (220 °C) is also due to the higher crystallinity of the fibers, as shown in Table 3. On the other hand, the UAIC exhibited a slightly lower thermal degradation temperature than ABC, which can be attributed to its lower crystallinity. During sonication, cavitation bubble collapse leads to extreme fiber damage. The crystalline portion of the fibers is broken and damaged as a result of the severe impact that occurs between the amorphous and crystalline sections of the fibers. As a result, the fibers' crystallinity is diminished, which lowers their thermal stability (Li *et al.* 2012). The third step corresponds to the degradation of carbonic residue into lower molecular weight

components, accompanied by the cleavage of glycosidic linkages in cellulose, resulting in weight losses of about 30.5% for ABC and 20.2% for UAIC.

As shown in Tables 1 and 2, based on FESEM analysis, the ABC samples had a length and diameter of 59.5 µm and 22.6 µm, respectively, while UAIC has a length and diameter of 77.8 µm and 32.9 µm, respectively. Therefore, the increased percentage of weight loss at this stage for ABC is attributed to its smaller fiber size compared to UAIC. Smaller fibers tend to degrade at slightly lower temperatures and consequently enhance char yield as reported by Li *et al.* (2012). Moreover, the gradual weight loss beyond 400 °C in UAIC sample is consistent with its larger size compared to ABC samples. These longer chains can contribute to the formation of a more extensive network of polyaromatic structures when the cellulose decomposes. This network can enhance the stability of the resulting char, making it more resistant to decomposition at higher temperatures. The generation of larger aromatic compounds and a more extensive cross-linked network take more energy to disintegrate. These structures contribute to the observed thermal degradation. Additionally, the surface area-to-volume ratio of larger cellulose particles is typically smaller, which may have an impact on how the material is exposed to heat and reactive gases during degradation and this could lead to a more stable and controlled degradation process.

CONCLUSIONS

1. This study presents compelling evidence of the successful isolation of cellulose from coconut shells using various investigated methods. The alkali and bleaching treatment (ABC) and the ultrasound-assisted alkali treatment (UAIC) proved effective in yielding cellulose from the coconut shells. Remarkably, UAIC demonstrated a higher cellulose yield compared to ABC. However, despite both methods yielding micro-sized particles, UAIC resulted in larger particles.
2. Ultrasonication played a crucial role in generating cellulose from raw material, owing to the physical effects of acoustic cavitation. These effects were primarily attributed to the asymmetrical implosion of cavitation microbubbles, leading to the generation of microjets near the plant surface. This, in turn, facilitated particle fragmentation, breaking down the cell wall of raw material and leading to the release of cellulose
3. While the hardness of coconut shells might have led researchers to believe that isolating cellulose would be challenging, current literature lacks the use of ultrasonic technology for these purposes. This research, however, demonstrated that the hardness of the coconut shell does not hinder cellulose isolation. The dense and lignin-rich structure of coconut shells presents physical obstacles that ultrasound technology can overcome, resulting in larger cellulose yields and improved quality. This makes ultrasound technology particularly attractive in this context. This study showed that ultrasonic isolation can improve the effectiveness of cellulose isolation while minimising processing time and energy usage. For this reason, it's a viable technique for handling difficult materials like coconut shells.
4. Further investigations such as chemical modifications or blending with other materials will make it possible to increase the isolated cellulose's quality. This work lays the groundwork for additional research and optimizations to address certain application requirements.

5. This study also showed that it is feasible to isolate cellulose from unconventional sources such as coconut shells, therefore expanding the range of raw materials available for cellulose manufacturing. This is a critical step that will support global sustainability efforts by lowering reliance on conventional wood-based sources.

ACKNOWLEDGMENTS

We want to thank the Ministry of Higher Education for the Fundamental Research Grant Scheme (FRGS/1/2022/STG04/UM/02/7) awarded to Dr. Nor Mas Mira Abd Rahman. The authors also gratefully acknowledge the financial support for part of this project from the Universiti Malaya under Bantuan Khas Penyelidikan / Special BKP (BKP002-2023-KP) and RU Grant SATU (ST043-2021).

REFERENCES CITED

Bano, S., and Negi, Y. S. (2017). "Studies on cellulose nanocrystals isolated from groundnut shells," *Carbohydrate Polymers* 157, 1041-1049. DOI: 10.1016/j.carbpol.2016.10.069

Chemat, F., Rombaut, N., Meullemiestre, A., Abert-vian, M., Sicaire, A.-G., and Fabiano-Tixier, A.-S. (2016). "Ultrasound assisted extraction of food and natural products. Mechanisms, techniques, combinations, protocols and applications. A review," *Ultrasonics Sonochemistry* 34, 540-560. DOI: 10.1016/j.ultsonch.2016.06.035

Chen, Y., Wu, Q., Huang, B., Huang, M., and Ai, X. (2015). "Isolation and characteristics of cellulose and nanocellulose from lotus leaf stalk agro-wastes," *BioResources* 10(1), 684-696. DOI: 10.15376/biores.10.1.684-696

Ching, Y. C., and Ng, T. S. (2014). "Effect of preparation conditions on cellulose from oil palm empty fruit bunch fiber," *BioResources* 9(4), 6373-6385. DOI: 10.15376/biores.9.4.6373-6385

Cichosz, S., and Masek, A. (2020). "IR study on cellulose with the varied moisture contents: Insight into the supramolecular structure," *Materials* 13(20), article 4573. DOI: 10.3390/ma13204573

Evans, S. K., Wesley, O. N., Nathan, O., and Moloto, M. J. (2019). "Chemically purified cellulose and its nanocrystals from sugarcane baggase: Isolation and characterization," *Heliyon* 5(10), article E02635. DOI: 10.1016/j.heliyon.2019.e02635

Gardner, D. J., Oporto, G. S., Mills, R., and Samir, M. A. S. A. (2008). "Adhesion and surface issues in cellulose and nanocellulose," *Journal of Adhesion Science and Technology* 22(5-6), 545-567. DOI: 10.1163/156856108X295509

Gupta, P. K., Raghunath, S. S., Prasanna, D. V., Venkat, P., Shree, V., Chithananthan, C., Choudhary, S., Surender, K., and Geetha, K. (2019). "An update on overview of cellulose , its structure and applications," in: *Cellulose,* InTechOpen. DOI: 10.5772/intechopen.84727

He, C., Li, H., Hong, J., Xiong, H., Ni, H., and Zheng, M. (2022). "Characterization and functionality of cellulose from pomelo fruitlets by different extraction methods," *Polymers* 14(3), article 518. DOI: 10.3390/polym14030518

Javanmard, A., Wan Daud, W. M. A., Patah, M. F. A., Zuki, F. M., Ai, S. P., Azman, D. Q., and Chen, W. H. (2024). "Breaking barriers for a green future: A comprehensive study on pre-treatment techniques for empty fruit bunches in the bio-based economy," *Process Safety and Environmental Protection* 182(November 2023), 535-558. DOI: 10.1016/j.psep.2023.11.053

Jerard, B. A., Damodaran, V., Jaisankar, I., Velmurugan, A., & Swarnam, T. P. (2018). Coconut biodiversity - nature's gift to the tropical islands. In *Biodiversity and Climate Change Adaptation in Tropical Islands* (pp. 145–185). Elsevier Inc. https://doi.org/10.1016/B978-0-12-813064-3.00006-5

Kalla, A. M., Franklin, M. E. E., Pushpadassa, H. A., Kumar, S., and Nath Battula, S. (2022). "Isolation and characterization of cellulose from coconut shell powder and its reinforcement in casein films," *The Pharma Innovation Journal* 11(10), 1043-1053. https://www.thepharmajournal.com/specialissue?year=2022&vol=11&issue=10S&ArticleId=16265

Kumar, A., Negi, Y. S., Choudhary, V., and Bhardwaj, N. K. (2014). "Characterization of cellulose nanocrystals produced by acid-hydrolysis from sugarcane bagasse as agro-waste," *Journal of Materials Physics and Chemistry* 2(1), 1-8. DOI: 10.12691/jmpc-2-1-1

Lavilla, I., and Bendicho, C. (2017). "Fundamentals of ultrasound-assisted extraction," in: *Water Extraction of Bioactive Compounds: From Plants to Drug Development*, Elsevier Inc., pp. 291-216. DOI: 10.1016/B978-0-12-809380-1.00011-5

Li, W., Yue, J., and Liu, S. (2012). "Preparation of nanocrystalline cellulose *via* ultrasound and its reinforcement capability for poly (vinyl alcohol) composites," *Ultrasonics Sonochemistry* 19(3), 479-485. DOI: 10.1016/j.ultsonch.2011.11.007

Liu, C., Li, B., Du, H., Lv, D., Zhang, Y., Yu, G., Mu, X., and Peng, H. (2016). "Properties of nanocellulose isolated from corncob residue using sulfuric acid, formic acid, oxidative and mechanical methods," *Carbohydrate Polymers* 151, 716-724. DOI: 10.1016/j.carbpol.2016.06.025

Madakson, P.,Yawas, D.S., and Apasi, A. (2012). "Characterization of coconut shell ash for potential utilization in metal matrix composites for automotive applications," *International Journal of Engineering Science and Technology* 4(3), 1190-1198.

Melikoğlu, A. Y., Bilek, S. E., and Cesur, S. (2019). "Optimum alkaline treatment parameters for the extraction of cellulose and production of cellulose nanocrystals from apple pomace," *Carbohydrate Polymers* 215, 330-337. DOI: 10.1016/j.carbpol.2019.03.103

Mohammed, M. A., Basirun, W. J., Abd Rahman, N. M. M., and Mohamad Salleh, N. (2021). "The effect of particle size of almond shell powders, temperature and time on the extraction of cellulose," *Journal of Natural Fibers*, 1-11. DOI: 10.1080/15440478.2021.1881689

Nayar, N. M. (2017). "The coconut in the world," in: *The Coconut*, pp. 1-8. DOI: 10.1016/b978-0-12-809778-6.00001-2

Ouarhim, W., Zari, N., Bouhfid, R., and el kacem Qaiss, A. (2019). "Mechanical performance of natural fibers based thermosetting composites," in: *Mechanical and Physical Testing of Biocomposites, Fiber-Reinforced Composites and Hybrid Composites*, Woodhead Publishing, Cambridge, UK, pp. 43-60.

Pasquini, D., de Morais Teixeira, E., da Siva Curvelo, A. A., Belgacem, M. N., and Dufresne, A. (2010). "Extraction of cellulose whiskers from cassava bagasse and their applications as reinforcing agent in natural rubber," *Industrial Crops and Products*

32(3), 486-490. DOI: 10.1016/j.indcrop.2010.06.022

Reddy, K. O., Ashok, B., Reddy, K. R. N., Feng, Y. E., Zhang, J., and Rajulu, A. V. (2011). "Extraction and characterization of novel ligno-cellulosic fibers from *Thespesia lampas* plant," *Mechanical Engineering Technology* 4(2), 1-20. DOI: 10.1080/1023666X.2014.854520

Rizal, W. A., Nisa, K., Maryana, R., Prasetyo, D. J., Pratiwi, D., Jatmiko, T. H., Ariani, D., and Suwanto, A. (2020). "Chemical composition of liquid smoke from coconut shell waste produced by SME in Rongkop Gunungkidul," *IOP Conference Series: Earth and Environmental Science* 462(1), 1-18. DOI: 10.1088/1755-1315/462/1/012057

Rodrigues, S., and Pinto, G. A. S. (2007). "Ultrasound extraction of phenolic compounds from coconut (*Cocos nucifera*) shell powder," *Journal of Food Engineering* 80(3), 869-872. DOI: 10.1016/j.jfoodeng.2006.08.009

Rosli, N. A., Ahmad, I., and Abdullah, I. (2013). "Isolation and characterization of cellulose nanocrystals from Agave angustofolia fiber," *BioResources* 8(2), 1893-1908. DOI: 10.15376/biores.8.2.1893-1908

Segal, L., Creely, J. J., Martin, A. E., and Conrad, C. M. (1959). "An empirical method for estimating the degree of crystallinity of native cellulose using the X-ray diffractometer," *Textile Research Journal* 29(10), 786-794. DOI: 10.1177/004051755902901003

Shokri, J., and Adibkia, K. (2013). "Application of cellulose and cellulose derivatives in pharmaceutical industries," in: *Cellulose - Medical, Pharmaceutical and Electronic Applications*, InTech, pp. 47-66. DOI: 10.5772/55178

Tangsathitkulchai, C., Junpirom, S., and Katesa, J. (2016). "Carbon dioxide adsorption in nanopores of coconut shell chars for pore characterization and the analysis of adsorption kinetics," *Journal of Nanomaterials* 1-10. DOI: 10.1155/2016/4292316

Theivasanthi, T., Anne Christma, F. L., Toyin, A. J., Gopinath, S. C. B., and Ravichandran, R. (2018). "Synthesis and characterization of cotton fiber-based nanocellulose," *International Journal of Biological Macromolecules* 109, 832-836. DOI: 10.1016/j.ijbiomac.2017.11.054

Wulandari, W. T., Rochliadi, A., and Arcana, I. M. (2016). "Nanocellulose prepared by acid hydrolysis of isolated cellulose from sugarcane bagasse," *IOP Conference Series: Materials Science and Engineering* 107, 832-836. DOI: 10.1088/1757-899X/107/1/012045

Yi, V. C. W., Yi, T. P., Xinxin, G., and Muei, C. L. (2019). "Ultrasonic-assisted alkaline extraction process to recover cellulose from sugarcane bagasse for carboxymethylcellulose production," *International Symposium on Green and Sustainable Technology* 2157(1), article 020044. DOI: 10.1063/1.5126579

Zhang, P. P., Tong, D. S., Lin, C. X., Yang, H. M., Zhong, Z. K., Yu, W. H., Wang, H., and Zhou, C. H. (2014). "Effects of acid treatments on bamboo cellulose nanocrystals," *Asia-Pacific Journal of Chemical Engineering* 9(5), 686-695. DOI: 10.1002/apj.1812

Article submitted: July 21, 2024; Peer review completed: August 7, 2024; Revised article received and accepted: August 21, 2024; Published: August 31, 2024.
DOI: 10.15376/biores.19.4.7870-7885